Author Manuscript

Author Manuscript

Author Manuscript

Author Manuscript

HHS Public Access

Author manuscript

Ann Surg. Author manuscript; available in PMC 2019 July 01.

Published in final edited form as:

Ann Surg. 2019 July ; 270(1): 180–187. doi:10.1097/SLA.0000000000002747.

STENT DESIGN AFFECTS FEMOROPOPLITEAL ARTERY DEFORMATION

Jason MacTaggart, MD[#1], **William Poulson, MD**[#1], **Andreas Seas, BS**[2], **Paul Deegan, MS**[1], **Carol Lomneth, PhD**[3], **Anastasia Desyatova, PhD**[1], **Kaspars Maleckis, PhD**[1], and **Alexey Kamenskiy, PhD**[1,**]

[1]University of Nebraska Medical Center, Omaha, NE

[2]Duke University, Durham, NC

[3]Creighton University, Omaha, NE

[#] These authors contributed equally to this work.

Abstract

Background: Poor durability of femoropopliteal artery (FPA) stenting is multifactorial, and severe FPA deformations occurring with limb flexion are likely involved. Different stent designs result in dissimilar stent-artery interactions, but the degree of these effects in the FPA is insufficiently understood.

Objectives: Determine how different stent designs affect limb flexion-induced FPA deformations.

Methods: Retrievable markers were deployed into n=28 FPAs of lightly embalmed human cadavers. Bodies were perfused and CT images were acquired with limbs in the standing, walking, sitting, and gardening postures. Image analysis allowed measurement of baseline FPA foreshortening, bending, and twisting associated with each posture. Markers were retrieved and seven different stents were deployed across the adductor hiatus in the same limbs. Markers were then re-deployed in the stented FPAs, and limbs were re-imaged. Baseline and stented FPA deformations were compared to determine the influence of each stent design.

Results: Proximal to the stent, Innova, Supera, and SmartFlex exacerbated foreshortening, SmartFlex exacerbated twisting, and SmartControl restricted bending of the FPA. Within the stent, all devices except Viabahn restricted foreshortening, Supera, SmartControl, and AbsolutePro restricted twisting, SmartFlex and Innova exacerbated twisting, and Supera and Viabahn restricted bending. Distal to the stents, all devices except AbsolutePro and Innova exacerbated foreshortening, and Viabahn, Supera, Zilver, and SmartControl exacerbated twisting. All stents except Supera were pinched in flexed limb postures.

[**]**CORRESPONDENCE AND REPRINTS REQUESTS TO:** Alexey Kamenskiy, Department of Surgery, 987690 Nebraska Medical Center, Omaha, NE 68198-7690, Tel: +1 (402) 559-5100, Fax: +1 (402) 559-8985, Alexey.Kamenskiy@unmc.edu.

DISCLOSURES

Authors declare that they have no conflict of interest in relation to this submission

Author Manuscript Author Manuscript Author Manuscript Author Manuscript

Conclusions: Peripheral self-expanding stents significantly affect limb flexion-induced FPA deformations, but in different ways. While certain designs appear to accommodate some deformation modes, no device was able to match all FPA deformations.

MINI ABSTRACT

We present head-to-head analysis of seven commonly used peripheral artery stents in a novel perfused human cadaver model. Results demonstrate that all stents significantly affect limb flexion-induced femoropopliteal artery deformations, but in different ways. No device was able to accommodate all deformation modes without restricting or exacerbating baseline arterial deformations.

Keywords

femoropopliteal artery; stenting; deformations; limb flexion; foreshortening; bending; twisting; pinching

1. INTRODUCTION

Atherosclerotic obstruction of the femoropopliteal artery (FPA) is associated with significant morbidity, mortality, and impairment in quality of life[1]. FPA stenting utilizing self-expanding nitinol stents is an increasingly popular, minimally-invasive procedure to improve arterial patency after angioplasty, particularly in cases involving more complex lesions and flow-limiting arterial dissections. Despite significant clinical experience and the availability of next generation stents, outcomes of the procedure continue to disappoint, with many patients developing reconstruction failure over a period of several months to a few years following stenting[2].

The ability of self-expanding stents to perform reasonably well in other arterial locations suggests that the local environment of the FPA plays a significant role in stent failure. Harsh mechanical conditions in the thigh and leg that induce significant foreshortening[3,4] (or axial compression), bending[3,5], twisting[6], and pinching[7] of the FPA likely produce adverse stent-artery interactions that may lead to restenosis or stent fracture. Recent data[3,5,6] suggest these deformations may be significantly more severe than previously assumed[7]. Furthermore, head-to-head bench-top tests[8] comparing FPA stents from different manufacturers demonstrated appreciable differences in device behavior between stent designs when subjected to different deformation modes and magnitudes.

Since bench-top tests currently cannot replicate the complex, multi-dimensional *in situ* loading conditions that exist in the FPA during limb flexion, these results need to be verified by more realistic models. While clinical data evaluating the comparative effectiveness of different stents is the ultimate gold standard, such analysis requires large sample sizes due to the heterogeneity of PAD patient populations, anatomical differences, and variability in lesion characteristics. Additionally, financial and logistical aspects of patient recruitment and device availability make head-to-head clinical comparisons of multiple stents challenging. Such analyses often limit endpoints to simple measures and are frequently insufficient to

Author Manuscript Author Manuscript Author Manuscript Author Manuscript

comprehensively characterize specific device behaviors, such as their ability to accommodate limb flexion-induced twisting[6].

We hypothesized that each of the seven stent designs would differentially affect limb flexion-induced FPA foreshortening, bending, twisting, and pinching. To test this hypothesis we used a perfused human cadaver model and intra-arterial marker method previously described and validated[3,5,6]. To allow a smaller sample size and reduce variability across cadavers and arteries, the same arteries were used to characterize both baseline and stented FPA deformations with each FPA acting as its own control.

2. METHODS

2.1 Baseline deformations with perfused human cadaver model

FPA deformations were measured using four-legged custom-designed nitinol intra-arterial markers depicted in Figure 1C. The markers were designed to move with the artery during limb flexion without sliding along its lumen or penetrating the FPA wall. One of the marker legs was made with extra material at the tip for easy identification on imaging, which allowed assessment of twisting that would otherwise be impossible to measure with sufficient resolution and accuracy. The head of each marker was hollow to allow insertion of a string for rapid marker deployment and retrieval. Prior to cadaver use, the marker technique was validated in silicone tubes and was found to produce accurate and repeatable measurements[6]. In cadavers validation was performed by imaging the arteries before and after marker deployment, with no measurable effect on limb flexion-induced deformations due to the presence of the markers (Figure 1).

A total of n=28 limbs from 15 lightly embalmed cadavers (average age 81±9 years old, range 60–93 years, 9 females, 6 males with no prior peripheral artery interventions, no aneurysmal disease, and no metal prostheses that would interfere with CT imaging) were used to assess FPA deformations with limb flexion. Use of lightly embalmed cadavers that were embalmed with glutaraldehyde-based solution as opposed to those that are fully embalmed with formaldehyde-based solution, allowed better preservation of natural tissue elasticity[9]. When compared to fresh human FPAs, lightly embalmed arteries resembled mechanical behavior of old and diseased FPAs (Figure 2), which was verified by performing planar biaxial extension testing[10–12] and comparing results to previously published data for fresh FPAs[13].

At least 10 hours before the experiment the limbs were wrapped with electric heating pads allowing the entire limb to heat up. During the procedure, angled catheter was inserted into either the posterior tibial or peroneal artery and then used to puncture the artery and surrounding soft tissues to establish through-and-through access for marker delivery and perfusion. Intra-arterial markers were compressed and loaded into a 6-French plastic tube for minimally invasive delivery into the FPA under fluoroscopic guidance from an external iliac artery access site. This allowed maintaining the integrity of the anatomical structures surrounding the FPA, while providing a sufficient number of reference points for accurate characterization of deformations. Depending on limb length approximately 22 markers

Author Manuscript Author Manuscript Author Manuscript Author Manuscript

spaced 2cm apart were deployed into each limb. More details describing this method are provided in our previous publications[3,5,6].

After marker delivery, FPAs were pressurized using a Harvard Apparatus Large Animal pump (Harvard Apparatus, Holliston, MA) circulating a 37°C radiopaque fluid containing calcium carbonate to avoid tissue swelling. Temperature of the perfusion fluid was measured exiting through the distal arterial end to ensure its consistency along the entire length of the artery.

Computerized Tomography images (GE Light Speed VCTXT scanner GE Healthcare, Waukesha, USA) of the limbs in the standing (180^{o}), walking (110^{o}), sitting (90^{o}), and gardening (60^{o}) postures were acquired with 0.625mm axial resolution to measure baseline deformations of the FPA with limb flexion (Figure 3).

2.2 Deformations of the FPA after stenting

After acquiring baseline images of the FPA in each limb posture, intra-arterial markers were retrieved through the same access site, and a single stent was deployed into each artery centered at the adductor hiatus with pre- and post-stent balloon dilatation. Stent diameters were chosen in accordance with manufacturer indications for use based on the baseline CT scan artery diameter measurements at the adductor hiatus. Seven stent designs with significantly different patterns (Figure 4B) were used in the study: AbsolutePro, Supera (both Abbott Vascular), Innova (Boston Scientific), Zilver (Cook Medical), SmartControl, SmartFlex (both Cordis), and Viabahn (GORE Medical). These stents were of three major types – conventional z-shape design (Absolute Pro, Innova, Zilver, SmartControl, SmartFlex), braided wire (Supera), and wrapped wire (Viabahn). Each of the seven stent designs was used in four limbs for a total of 28 stented limbs. After stenting, markers were redeployed into the stented FPAs, and CT images were again obtained with limbs in the standing, walking, sitting, and gardening postures. An example of a baseline and stented FPA is demonstrated in Figure 4C.

A total of 224 three-dimensional CT reconstructions (Figure 3) were performed with Mimics (Materialise, Leuven, Belgium) software using a combination of region growing and segmentation tools[3,6] by a single operator to reduce variability. Limb flexion-induced arterial deformations before and after stenting were measured using these reconstructions in three segments along the FPA length: proximal to the stent, within the stented segment, and distal to the stented segment (Figure 4A). Techniques for measuring foreshortening, bending, and twisting are described in our previous works[3,6] and are illustrated in Figure 5. Briefly, foreshortening due to limb flexion was measured as change in distance between each pair of markers in the straight and flexed postures along the arterial centerline. Bending was measured by manually inscribing best-fit spheres to the FPA centerline and recording their diameters (i.e. smaller diameters indicated more severe bends). Twisting was measured as difference in rotation between two consecutive markers in the straight and flexed postures. This rotation difference was normalized to the distance between the markers to obtain a per-centimeter twist value. This step was important because rotation of say 90° over 1cm is significantly more severe than 90° twist distributed over a 2cm distance. Finally,

Author Manuscript Author Manuscript Author Manuscript Author Manuscript

cross-sectional pinching was measured in the stented artery as the ratio of major to minor axes of the elliptical cross-section at the most pinched location.

Effects of stenting on baseline deformations were assessed by calculating differences in foreshortening, bending, and twisting between baseline and stented arteries expressed as percent of baseline deformations. Two-tailed paired t-tests were used to assess statistical significance of findings and in order to compare the overall effects of each stent type, a combined mechanical compatibility score (CMCS) was introduced. This score included statistically significant exacerbation of deformations proximal, within, and distal to the stented segment.

3. RESULTS

3.1 Foreshortening

Maximum baseline foreshortening was 9–15% in the SFA, 11–19% at the AH, and 13–25% in the PA depending on posture[3]. Foreshortening of the FPA proximal to the segment that was later stented was 3–6%, and foreshortening within and distal to the segment that was later stented was 7–14% depending on posture. Effects of stenting on baseline foreshortening are presented in Figure 6A. Results are organized by stent type and demonstrate the effects observed proximal, within, and distal to the stented segments. Positive values indicate that arterial segment foreshortened more after stenting, i.e. foreshortening was exacerbated. Negative values indicate that the segment foreshortened less after stenting, i.e. the stent restricted baseline axial deformations.

Overall, most stents exacerbated foreshortening proximal and distal to the stent, but restricted foreshortening within the stented segment. Proximal to the stented segment, Innova (71%), Supera (34%), and SmartFlex (15%) exacerbated baseline foreshortening, while effects of other stents did not reach statistical significance. Within the stented segment, all stents except Viabahn restricted FPA foreshortening with largest restriction produced by SmartControl (54%) and SmartFlex (46%) stents, followed by Zilver (41%), Supera (28%), AbsolutePro (22%) and Innova (15%) stents. Distal to the stented segment SmartControl (49%), SmartFlex (39%), Zilver (39%), Viabahn (31%) and Supera (21%) stents exacerbated baseline foreshortening.

3.2 Bending

Maximum bending of the SFA expressed as radii of inscribed spheres ranged from 21–27mm, bending of the artery at the AH was 9–19mm, and bending of the PA was 8–17mm depending on posture[3]. Baseline bending radii in the FPA proximal to the segment of the artery that was later stented ranged from 18–23mm, within the segment that was later stented 5–14mm, and distal to the segment that was later stented 5–11mm depending on posture. Effects of stenting on FPA bending are presented in Figure 6B. Negative values indicate that arterial segment was bending more with limb flexion after stenting, while positive values indicate that it was bending less, i.e. became straighter after stenting.

Proximal to the stented segment, the SmartControl stent restricted baseline bending by 96%, while effects of other stents were not statistically significant. Within the stented segment,

Author Manuscript Author Manuscript Author Manuscript Author Manuscript

Supera (75%) and Viabahn (74%) restricted bending, making the stented segment straighter during limb flexion. Although SmartControl also straightened the stented segment of the FPA, this result was not statistically significant (p=0.12) due to a large standard deviation. No statistically significant effects were observed distal to the stented segment.

3.3 Twisting

Maximum baseline twisting observed in the SFA ranged from 10–13°/cm, 8–16°/cm at the AH, and in the PA 14–26°/cm depending on posture[6]. Maximum baseline twisting in the FPA proximal to the segment that was later stented ranged from 10 to 14°/cm, within the segment that was later stented 11–21°/cm, and distal to the segment that was later stented 10–18°/cm depending on posture. Effects of stenting on baseline twisting are summarized in Figure 6C. Positive values indicate that limb flexion-induced twisting was exacerbated after stenting, while negative values show the opposite.

Proximal to the stented segment, SmartFlex (57%) exacerbated limb flexion-induced twisting, but no statistically significant effects were observed for other devices. Within the stented segment the largest exacerbation of FPA twisting was also produced by SmartFlex (113%), followed by Innova (83%). Supera (47%), SmartControl (34%), and AbsolutePro (30%) restricted FPA twisting within the stented segment. Distal to the stented segment, Viabahn (77%), Supera (59%), Zilver (35%) and SmartControl (31%) exacerbated limb flexion-induced FPA twisting.

3.4 Pinching

All stents except Supera were pinched by limb flexion-induced deformations. The degree of pinching for each stent design is presented in Figure 6D. The SmartControl (1.34) stent was pinched the most, followed by Innova (1.30), AbsolutePro (1.22), Viabahn (1.18), Zilver (1.15), and SmartFlex (1.06) devices. In most cases highest pinching was observed at the Adductor Hiatus.

3.5 Overall comparison - combined mechanical compatibility score (CMCS)

Figure 7 summarizes the effects of all deformation modes on limb flexion-induced deformations using a Combined Mechanical Compatibility Score (CMCS). Since it is not yet clear which deformations play more important roles in pathophysiology, all were given the same weight. Different colors represent different deformation modes that were either exacerbated (positive values) or restricted (negative values) by stenting, and patterns indicate segments of the artery where these deformations were measured. Overall, none of the stents accommodated all FPA deformations, largest exacerbation was produced by the SmartFlex stent, while Supera was the most mechanically compatible. The largest overall restriction of FPA deformations was produced by the SmartControl stent, while AbsolutePro restricted these deformations the least.

4. DISCUSSION

The femoropopliteal artery experiences complex mechanical deformations with limb flexion and extension. These deformations include foreshortening, bending, twisting, and pinching

Author Manuscript Author Manuscript Author Manuscript Author Manuscript

of the artery that vary depending on limb posture and anatomic location[3,5–7,14–16]. Deformation severity has recently been quantified using a perfused human cadaver model and intra-arterial marker technique. Although not considering active muscle contractions, perfused human cadaver models are able to simulate many complexities of the FPA environment and therefore are a viable alternative for characterization of artery-endovascular device interaction[17,18]. Recent studies using these models have demonstrated that FPA deformations are primarily localized to the SFA at the adductor hiatus and the popliteal artery below the knee, and are significantly more severe than assumed previously[3,5–7]. These studies further suggest that currently available PAD stents may not properly accommodate these deformations, which indeed has been demonstrated by a recent bench-top comparison of 12 commercially available PAD stents. In this study by Maleckis[8], most PAD stents were not able to withstand foreshortening, bending, and twisting experienced by the FPA without buckling. While bench-top stent testing allows understanding of device design features that contribute to their performance, these tests are not able to replicate the complexities of FPA loading environments and the interplay between the artery and the stent. To better understand this issue, our current study compared the influence of seven PAD stent designs on limb flexion-induced FPA deformations using the cadaver model, employing each artery as its own control to isolate the effect of each stent on baseline arterial deformations.

Our data demonstrate that all seven stent designs significantly influence limb flexion-induced FPA deformations, not only within the stented segment, but also proximal and distal to it. Stent design features likely influence these stent-artery interactions. Braided and z-shaped designs, strut length, width, thickness and number, as well as geometry of interconnections and properties of the nitinol material, all interact to produce measurable differences in stent behavior, and appear to exert major effects on the ability of the device to accommodate limb flexion-induced deformations.

No stent appears to accommodate all deformation modes without either exacerbating or restricting baseline deformations. Restriction of foreshortening within the stented segment observed in this study agrees with previous findings in patient[4,19], cadaver[20], and computational models[21], and the amount of restriction for different devices correlates with device stiffness in compression determined with bench-top tests[8]. In these tests the Viabahn stent-graft restricted foreshortening the least, likely due to its helically wrapped wire around specially designed PTFE fabric, while most other devices contained multiple, rigid longitudinal connectors that restricted foreshortening.

Bending stiffness also significantly affected performance of stents in the cadaver model. The SmartControl stent had the highest bending stiffness in bench-top experiments[8], and it also produced the largest restriction of FPA bending in our cadaver model (Figure 6B). Braided-wire and wrapped-wire stents on the other hand demonstrated more gentle curvatures in bench-top experiments (Figure 8), and produced less acute bending in situ. Effects of bending stiffness on curvature have been previously reported in cadaver models[20] and PAD patients[4] where kinks similar to those described in Figure 4C were observed at the distal end of some stents.

Author Manuscript Author Manuscript Author Manuscript Author Manuscript

While foreshortening and bending can be quantified without the use of intra-arterial markers[19,20], these markers are essential for accurate quantification of FPA twisting with limb flexion[6]. Our data demonstrate that stent design has significant effects on FPA twisting, and results are again in good agreement with bench-top data on torsional stiffness[8]. Interestingly, though some stents restricted twisting within the stented segment, they exacerbated it distally. Restriction of twist appears to be related to friction between the wires in braided stents, and the short longitudinal strut connections in conventional z-shape stents. The fact that twisting was exacerbated distally suggests that if the FPA twist cannot be accommodated by the stent due to its high torsional stiffness, it may be translated proximal or distal to the device, resulting in exacerbation of FPA torsion. This could be the mechanism leading to the so-called “candy wrapper” edge restenosis seen with certain stents[22]. In some devices, like the SmartFlex, twists were exacerbated in multiple segments, likely due to the unique spiral design of these stents that endows them with coupled axial-torsional characteristics[8]. Since the FPA exhibits combined twisting and axial foreshortening with limb flexion, spiral stents can exacerbate both.

Finally, radial stiffness appeared to have paramount effects on stent pinching due to limb flexion. In bench-top experiments, the Supera stent demonstrated radial stiffness at least an order of magnitude higher than the radial stiffness of any other device, likely due to its braided design and frictional forces between the wires. Supera was also the only stent that was not pinched by limb flexion-induced deformations in our cadaver model. The radial stiffness of the Supera stent appears to be profoundly influenced by proper stent deployment technique with nominally deployed stents producing a braid angle that strongly resists radial compression, while maldeployed elongated Supera stents are radially weak. On the contrary, z-shaped stents, particularly those that contained large number of heavily connected short struts, had trouble accommodating bending deformations, which resulted in significant pinching (Figure 8) that could potentially affect flow patterns and cause stent malapposition during limb flexion.

While our data demonstrate appreciable differences in how different stent designs affect limb flexion-induced FPA deformations, they are not intended to suggest clinical superiority of one stent versus another. These results represent a purely mechanical evaluation of stent characteristics that should be viewed in the context of the study’s limitations. First and foremost, cadaver models cannot perfectly recapitulate live tissue responses, which likely play a central role in PAD pathophysiology. Ultimately, stent performance must be judged by clinical trials[23], rather than bench-top or cadaver experiments, though these supplementary assessments may help in the interpretation of clinical differences observed between devices and guide optimization of future designs. The other limitation of this work is the lack of stent fatigue and fracture assessments. Since FPA stents function in one of the most dynamic environments in the vasculature, they also have one of the highest fracture rates[24] correlating with exercise frequency[25]. While the incidence of material fatigue and stent fracture appears to be much more frequent in FPA stents than in carotid or iliac stents, it is likely not the only factor contributing to reconstruction failure as most patients with FPA restenosis do not have fractures in their stents[26]. Nevertheless, resistance of FPA stents to fracture is an important characteristic that is unlikely to be studied using a cadaver model due to lengthy multi-million-cycle experiments required to characterize fatigue. Other

Author Manuscript Author Manuscript Author Manuscript Author Manuscript

mechanical characteristics not considered in this study may also have important roles in stent performance[27,28]. Stent abrasiveness, for example, may have paramount influence on the artery wall with the “gator-back” appearance of certain devices seen during bending possibly contributing to this process (Figure 8). Finally, though the present findings demonstrate appreciable differences in mechanical behavior of PAD stents, these differences cannot be attributed to a single design feature, like the strut thickness, number of interconnectors, braid angle or the like. Parametric computational studies on each device are required to understand how each design feature contributes to the overall stent behavior. Consideration of these additional characteristics and validation of these findings with patient data will be the focus of future studies. In the meantime, presented results may help stent manufacturers optimize their devices for better mechanical compatibility with limb flexion-induced FPA deformations.

5. CONCLUSIONS

We evaluated PAD stents for their differential abilities to handle the severe deformations that the FPA experiences with limb flexion. The SmartControl and SmartFlex stents influence limb flexion-induced deformations more than other stent designs, corroborating bench-top conclusions[8]. The Supera stent exacerbated baseline FPA deformations the least, while the AbsolutePro had overall the least influence in terms of both restriction and exacerbation. While exacerbation of already large deformations by stents is unlikely to benefit FPA healing, it is yet to be understood whether restriction of these deformations is positive or negative for optimal arterial function and healing. On one hand, straighter arterial segments produced by stiffer stents may contribute to more laminar flow patterns, while this characteristic can also be associated with high stress concentrations at the stent ends as the artery conforms around more rigid devices during limb flexion. High stress concentrations can damage the arterial wall and may lead to deleterious cellular and biochemical responses culminating in reconstruction failure[5,29–32]. More research utilizing live patient and large animal data will be required to determine the influence of these factors on arterial healing.

Acknowledgments

FUNDING

Research reported in this publication was supported in part by the National Heart, Lung, And Blood Institute of the National Institutes of Health under Award Numbers R01 HL125736 and F32 HL124905.

6. REFERENCES

1. Fowkes FGR, Rudan D, Rudan I, et al. Comparison of global estimates of prevalence and risk factors for peripheral artery disease in 2000 and 2010: a systematic review and analysis. Lancet. 2013;6736:1–12.
2. Schillinger M, Sabeti S, Dick P, et al. Sustained benefit at 2 years of primary femoropopliteal stenting compared with balloon angioplasty with optional stenting. Circulation. 2007;115:2745–9. [PubMed: 17502568]
3. Poulson W, Kamenskiy A, Seas A, et al. Limb flexion-induced axial compression and bending in human femoropopliteal artery segments. J Vasc Surg 2017;1–7.
4. Gökgöl C, Schumann S, Diehm N, et al. In Vivo Quantification of the Deformations of the Femoropopliteal Segment. J Endovasc Ther 2017;24:27–34. [PubMed: 28095767]

Author Manuscript Author Manuscript Author Manuscript Author Manuscript

5. MacTaggart JJN, Phillips NNY, Lomneth CCS, et al. Three-Dimensional Bending, Torsion and Axial Compression of the Femoropopliteal Artery During Limb Flexion. J Biomech 2014;47:2249–2256. [PubMed: 24856888]
6. Desyatova A, Poulson W, Deegan P, et al. Limb flexion-induced twist and associated intramural stresses In the human femoropopliteal artery. J R Soc Interface;14 Epub ahead of print 2017. DOI: 10.1098/rsif.2017.0025.
7. Ansari F, Pack LK, Brooks SS, et al. Design considerations for studies of the biomechanical environment of the femoropopliteal arteries. J Vasc Surg 2013;58:804–813. [PubMed: 23870198]
8. Maleckis K, Deegan P, Poulson W, et al. Comparison of Femoropopliteal Artery Stents Under Axial and Radial Compression, Axial Tension, Bending, and Torsion Deformations. J Mech Behav Biomed Mater. 2017;75:Available online 13 July 2017.
9. Wadman MC, Lomneth CS, Hoffman LH, et al. Assessment of a new model for femoral ultrasound-guided central venous access procedural training: a pilot study. Acad Emerg Med 2010;17:88–92. [PubMed: 20003122]
10. Kamenskiy A, Pipinos I, Dzenis Y, et al. Passive biaxial mechanical properties and in vivo axial pre-stretch of the diseased human femoropopliteal and tibial arteries. Acta Biomater. 2014;10:1301–1313. [PubMed: 24370640]
11. Kamenskiy A, Seas A, Bowen G, et al. In situ longitudinal pre-stretch in the human femoropopliteal artery. Acta Biomater. 2016;32:231–237. [PubMed: 26766633]
12. Kamenskiy AV, Pipinos II, Dzenis YA, et al. Effects of age on the physiological and mechanical characteristics of human femoropopliteal arteries. Acta Biomater. 2015;11:304–13. [PubMed: 25301303]
13. Kamenskiy A, Seas A, Deegan P, et al. Constitutive description of human femoropopliteal artery aging. Biomech Model Mechanobiol 2017;16:681–692. [PubMed: 27771811]
14. Cheng C, Wilson N, Hallett R. In vivo MR angiographic quantification of axial and twisting deformations of the superficial femoral artery resulting from maximum hip and knee flexion. J Vasc Interv Radiol 2006;17:979–987. [PubMed: 16778231]
15. Cheng CP, Choi G, Herfkens RJ, et al. The effect of aging on deformations of the superficial femoral artery resulting from hip and knee flexion: potential clinical implications. J Vasc Interv Radiol 2010;21:195–202. [PubMed: 20022767]
16. Klein AJ, Chen SJ, Messenger JC, et al. Quantitative assessment of the conformational change in the femoropopliteal artery with leg movement. Catheter Cardiovasc Interv 2009;74:787–798. [PubMed: 19521998]
17. Nikanorov A, Smouse HB, Osman K, et al. Fracture of self-expanding nitinol stents stressed in vitro under simulated intravascular conditions. J Vasc Surg 2008;48:435–440. [PubMed: 18486426]
18. Arbatli H, Cikirikcioglu M, Pektok E, et al. Dynamic Human Cadaver Model for Testing the Feasibility of New Endovascular Techniques and Tools. Ann Vasc Surg 2010;24:419–422. [PubMed: 19619977]
19. Nikanorov A, Schillinger M, Zhao H, et al. Assessment of self-expanding nitinol stent deformation after chronic implantation into the femoropopliteal arteries. EuroIntervention. 2013;9:730–737. [PubMed: 24169133]
20. Ni Ghriallais R, Heraty K, Smouse B, et al. Deformation of the Femoropopliteal Segment: Effect of Stent Length, Location, Flexibility, and Curvature. J Endovasc Ther 2016;23:907–918. [PubMed: 27647689]
21. Ní Ghriallais R, Bruzzi M. A computational analysis of the deformation of the femoropopliteal artery with stenting. J Biomech Eng 2014;136:1–10.
22. Geraghty PJ. Covered stenting of the superficial femoral artery using the Viabahn stent-graft. Perspect Vasc Surg Endovasc Ther 2006;18:39–43. [PubMed: 16628330]
23. Treitl KM, Woerner B, Schinner R, et al. Evolution of patency rates of self-expandable bare metal stents for endovascular treatment of femoro-popliteal arterial occlusive disease: Does stent design matter? Eur Radiol 2017;27:3947–3955. [PubMed: 28168366]

Author Manuscript Author Manuscript Author Manuscript Author Manuscript

24. Higashiura W, Kubota Y, Sakaguchi S, et al. Prevalence, factors, and clinical impact of self-expanding stent fractures following iliac artery stenting. J Vasc Surg 2009;49:645–652. [PubMed: 19268770]

25. Iida O, Nanto S, Uematsu M, et al. Effect of exercise on frequency of stent fracture in the superficial femoral artery. Am J Cardiol 2006;98:272–274. [PubMed: 16828607]

26. Kurayev A, Zavlunova S, Babaev A. CRT-207 Role of Nitinol Stent Fractures in the Development of In-Stent Restenosis in the Superficial Femoral Artery. JACC Cardiovasc Interv 2014;7:S35.

27. Maleckis K, Anttila E, Aylward P, et al. Nitinol Stents In The Femoropopliteal Artery: A Mechanical Perspective on Material, Design, and Performance. Ann Biomed Eng.;Accepted.

28. Stoeckel D, Pelton A, Duerig T. Self-expanding nitinol stents: material and design considerations. Eur Radiol 2004;14:292–301. [PubMed: 12955452]

29. Clowes AW, Reidy MA, Clowes MM. Mechanisms of stenosis after arterial injury. Lab Invest 1983;49:208–215. [PubMed: 6876748]

30. Wensing PJW, Meiss L, Mali WPTM, et al. Early Atherosclerotic Lesions Spiraling Through the Femoral Artery. Arterioscler Thromb Vasc Biol 1998;18:1554–1558. [PubMed: 9763526]

31. Dunlop GR, Santos R. Adductor-Canal Thrombosis. N Engl J Med 1957;256:577–580. [PubMed: 13451898]

32. Watt J Origin of femoro-popliteal occlusions. Br Med J 1965;2:1455–1459. [PubMed: 5849435]

Author Manuscript Author Manuscript Author Manuscript Author Manuscript

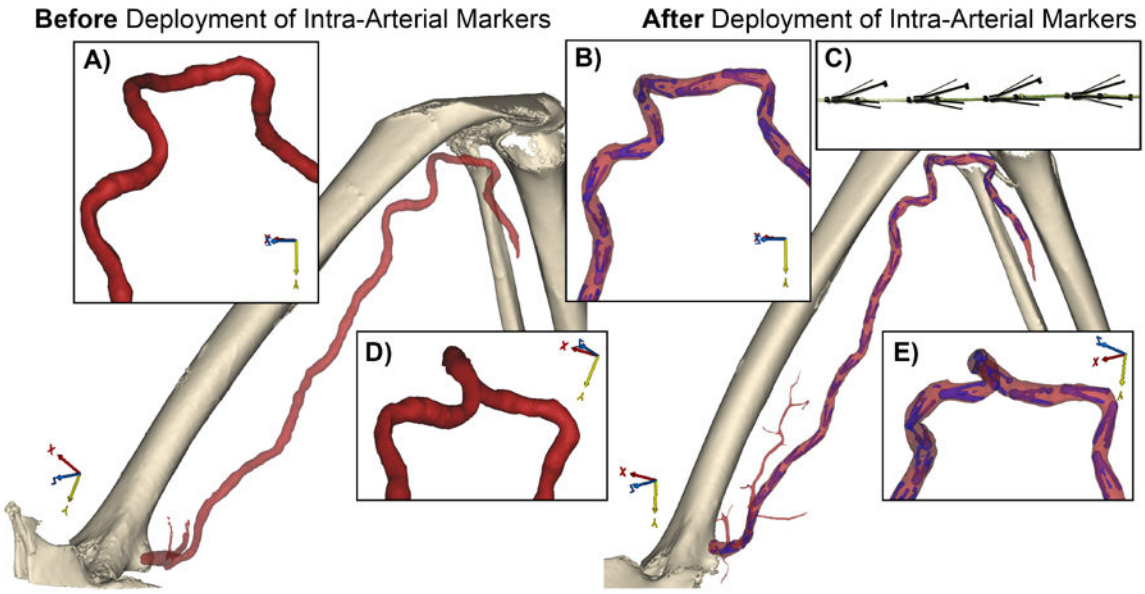

Figure 1.

Representative image of the FPA in the gardening posture before (A,D) and after (B,E) deployment of intra-arterial markers (C). Inserts demonstrate magnified views of the FPA in different projections illustrating that markers did not influence natural deformations of the artery with limb flexion.

Author Manuscript Author Manuscript Author Manuscript Author Manuscript

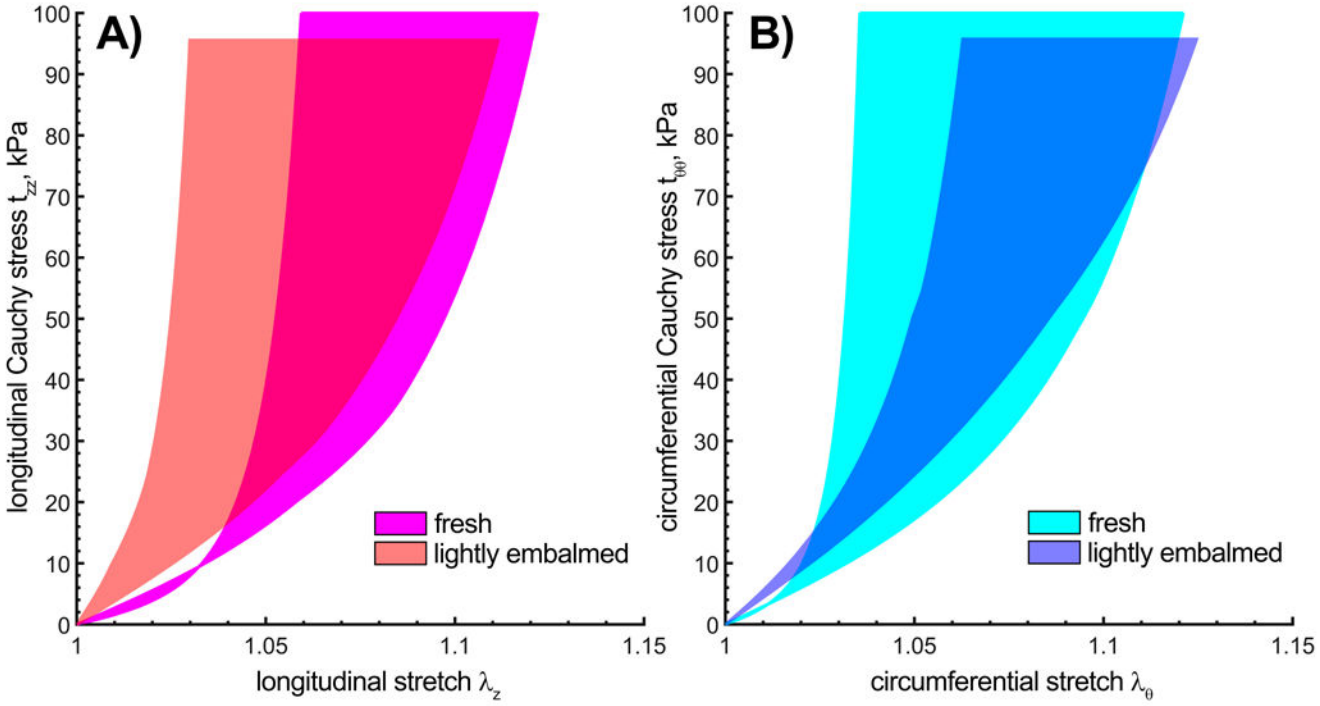

Figure 2.

Ranges of femoropopliteal artery mechanical properties in longitudinal (A) and circumferential (B) directions from lightly embalmed arteries used in this study (age 81±9 years, n=15) compared to mechanical properties of fresh cadaveric femoropopliteal arteries (age 78±2 years, n=15) tested previously[13]. Ranges bound 25th and 75th percentiles. Note that some lightly embalmed tissues were somewhat stiffer in the longitudinal direction, possibly due to older age.

Author Manuscript Author Manuscript Author Manuscript Author Manuscript

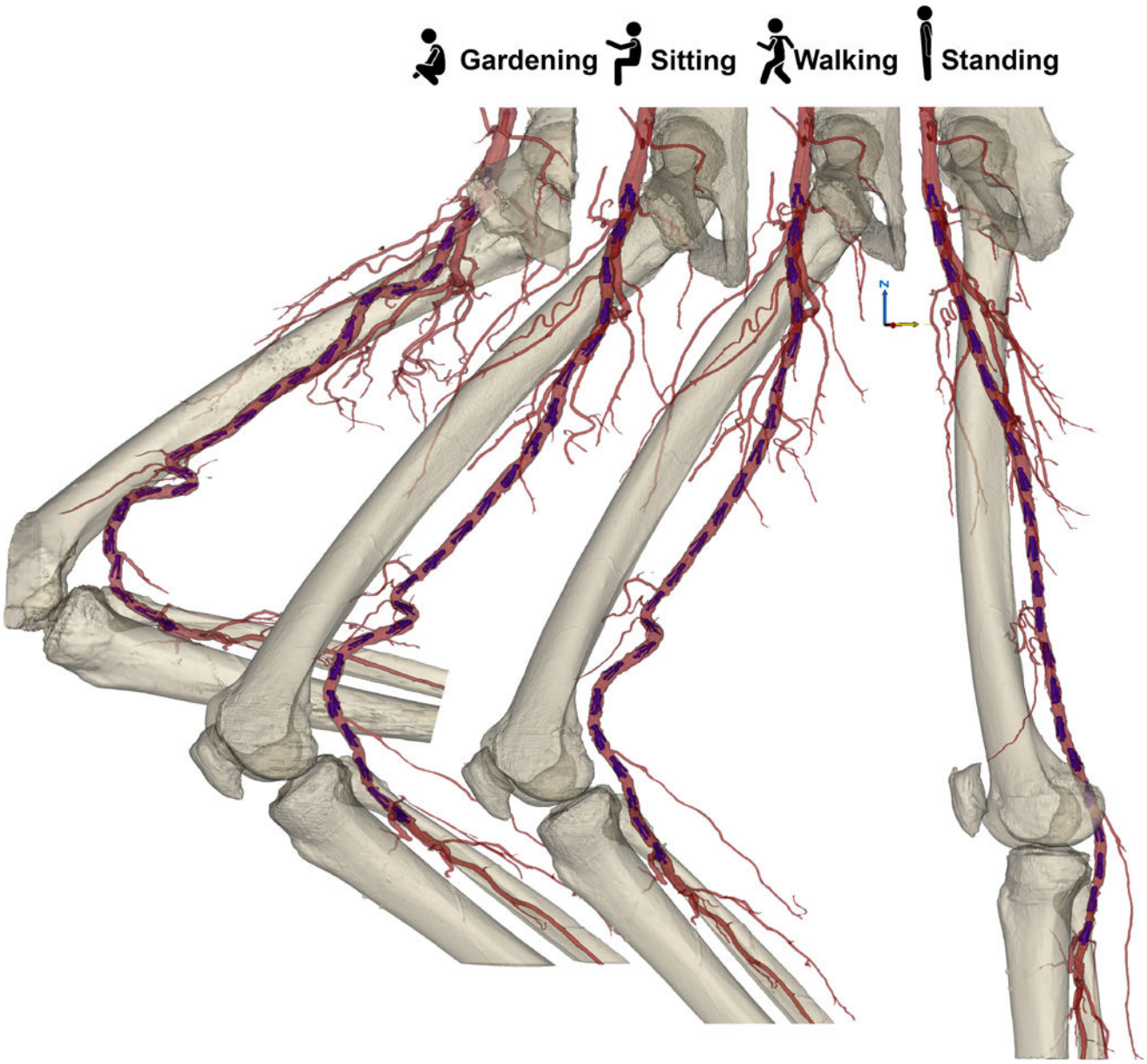

Figure 3.
Three-dimensional reconstructions of femoropopliteal artery deformations due to limb flexion derived from CT imaging of the limb in standing, walking, sitting, and gardening postures.

Author Manuscript Author Manuscript Author Manuscript Author Manuscript

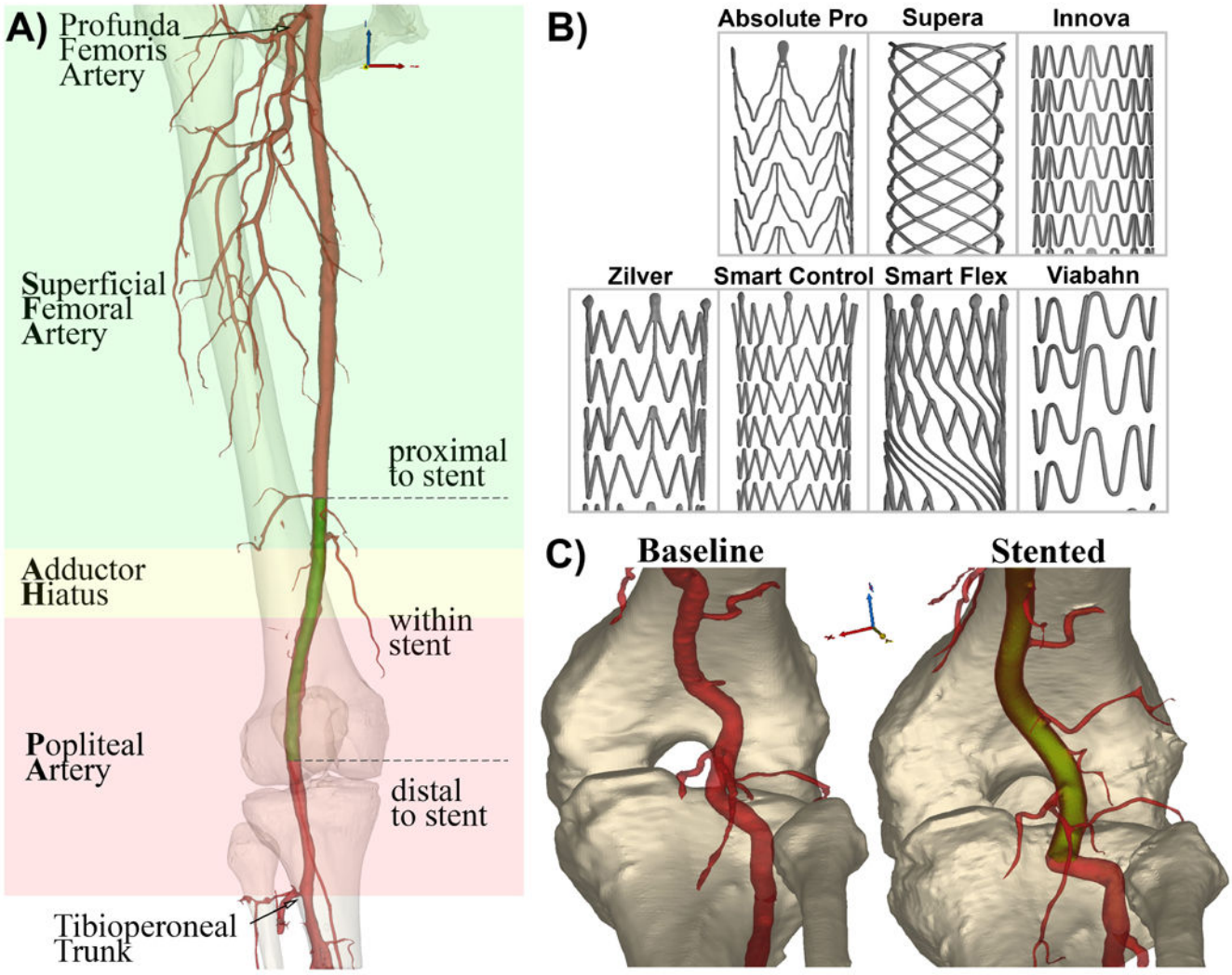

Figure 4.

A) Stented femoropopliteal artery consisting of the proximal superficial femoral artery (SFA), adductor hiatus (AH) segment, and popliteal artery (PA). Stent is colored green; B) design patters of seven stents used in the study; C) example of an FPA below the knee before and after stenting.

Author Manuscript Author Manuscript Author Manuscript Author Manuscript

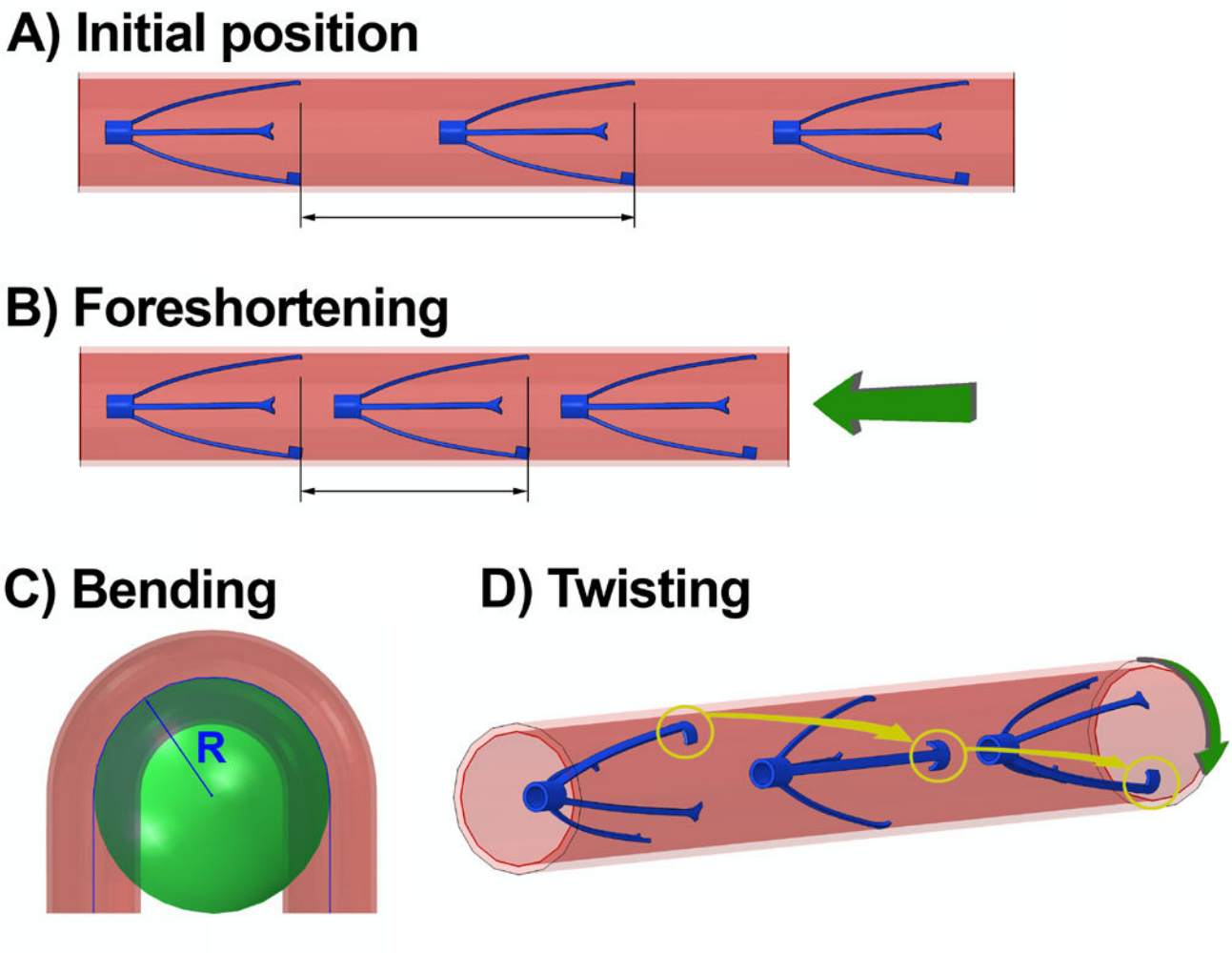

Figure 5.
Illustration of the method to measure femoropopliteal artery deformations with limb flexion demonstrating intra-arterial markers in the undeformed artery (A). Markers were used to measure FPA foreshortening (B) and twisting (D), while centerline was used to assess bending (C).

Author Manuscript
Author Manuscript
Author Manuscript
Author Manuscript

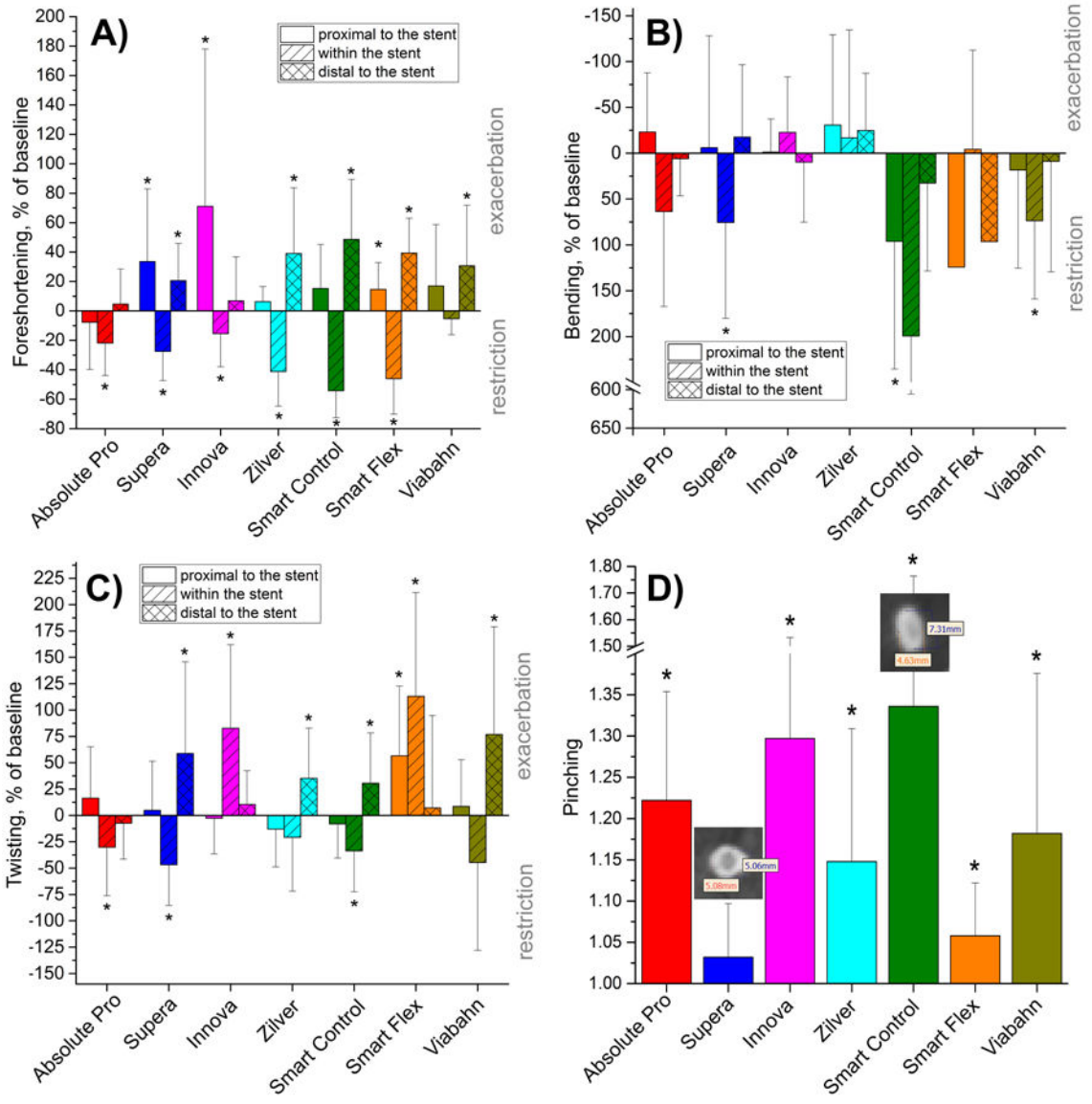

Figure 6.

Effects of stenting on A) foreshortening, B) bending, C) twisting, and D) pinching of the FPA proximal, within, and distal to the stented segment expressed as percentage of baseline deformations. Values above the horizontal axis indicate that stent exacerbated baseline deformations, while values below the horizontal axis indicate that stent restricted baseline deformations. Statistically significant results ($p<0.05$) are marked with an asterisk. Error bars demonstrate standard deviations. Note that restriction and exacerbation often occurs sequentially proximal, within, and distal to the stented segment. In panel D) larger values indicate larger deviation from a perfectly circular cross-section.

Author Manuscript Author Manuscript Author Manuscript Author Manuscript

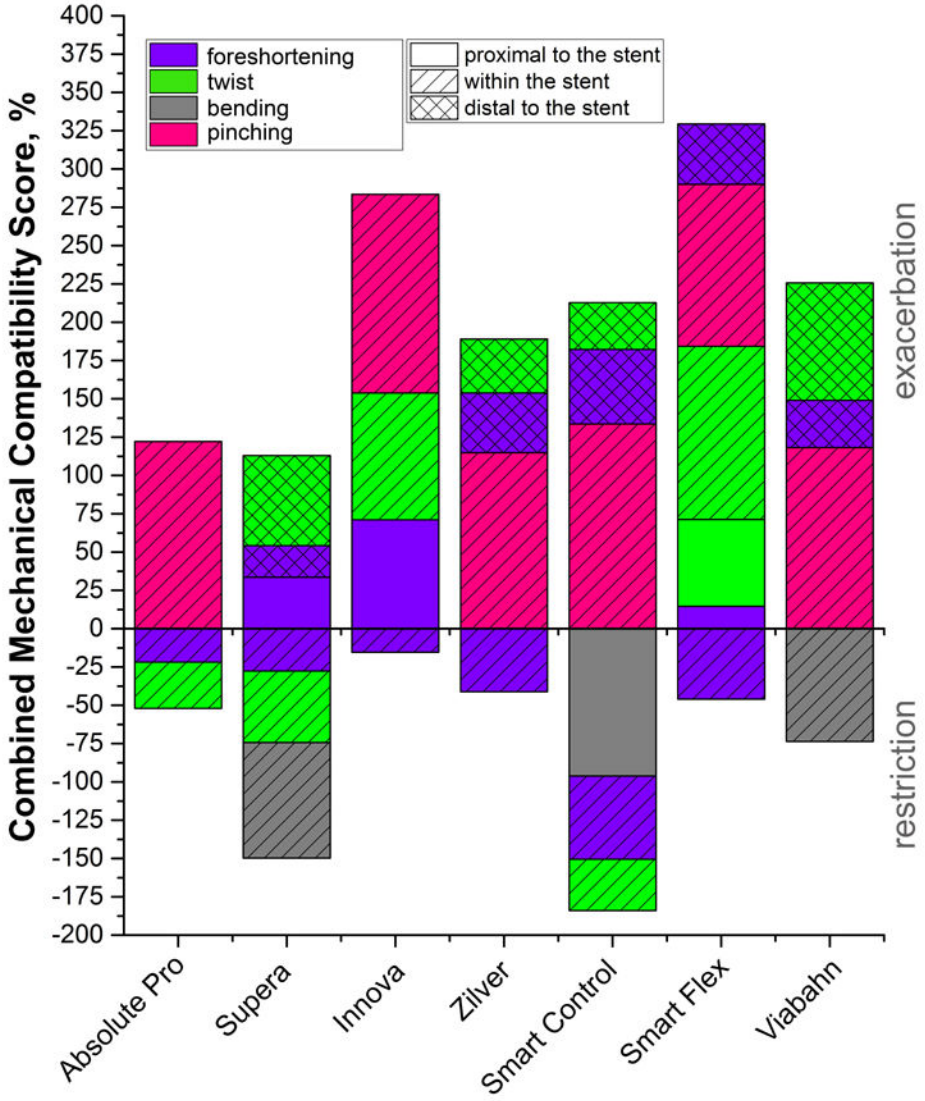

Figure 7.

Combined Mechanical Compatibility Score (CMCS, %) for seven FPA stents summarizing their effects on limb flexion-induced FPA deformations. Only statistically significant effects are included. Different colors represent different deformation modes, while patterns indicate the segment of the artery in which they were measured. Positive values indicate exacerbation of baseline deformations, while negative values indicate restriction. Note that none of the stents exacerbated baseline bending, but some restricted it.

Author Manuscript Author Manuscript Author Manuscript Author Manuscript

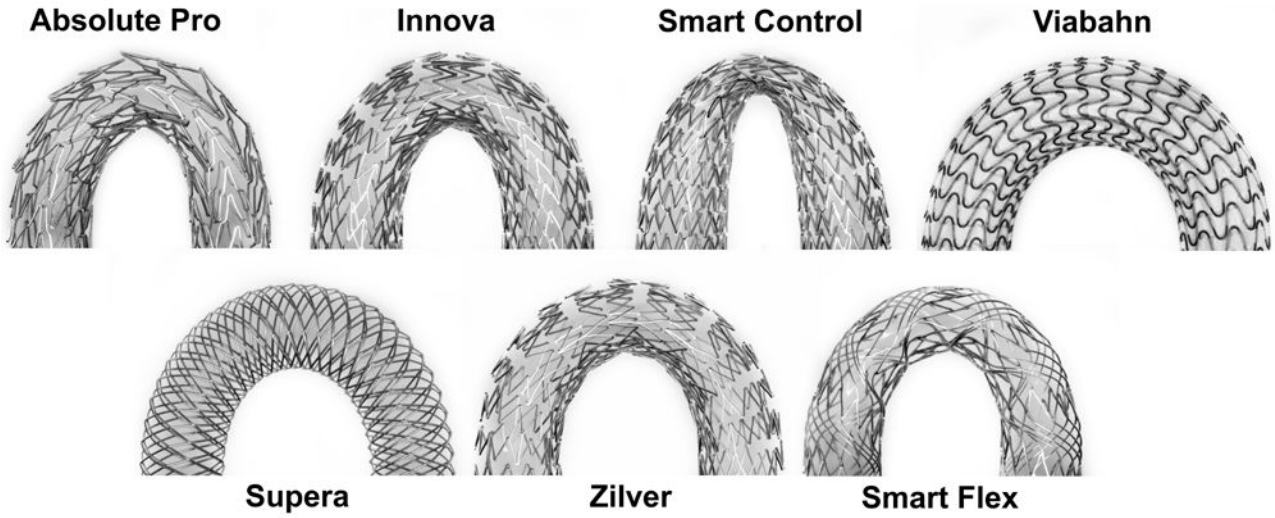

Figure 8.

Pinching of stents due to bending. Note the significant pinching of the SmartControl stent. Also note the “gator-back” appearance of the Absolute Pro with strut apices pointing away from the bend and towards the arterial wall.